Journal of ELECTRICAL ENGINEERING, VOL. 54, NO. 1-2, 2003, 13–21

NEURAL NETWORK MODEL FOR SCALAR AND VECTOR HYSTERESIS

Miklós Kuczmann — Amália Iványi *

The Preisach model allows to simulate the behaviour of magnetic materials including hysteresis phenomena. It assumes that ferromagnetic materials consist of many elementary interacting domains, and each of them can be represented by a rectangular elementary hysteresis loop. The fundamental concepts of the Preisach model is that different domains have some probability, which can be described by a distribution function, also called the Preisach kernel. On the basis of the so-called Kolmogorov-Arnold theory the feedforward type artificial neural networks are able to approximate any kind of non-linear, continuous functions represented by their discrete set of measurements. A neural network (NN)based scalar hysteresis model has been constructed on the function approximation ability of NNs and if-then type rules about hysteresis phenomena. Vectorial generalization to describe isotropic and anisotropic magnetic materials in two and three dimensions with an original identification method has been introduced in this paper. Good agreement is found between simulated and experimental data and the results are illustrated in figures.

K e y w o r d s: hysteresis characteristics, Everett surface, vector hysteresis, feedforward type neural networks, backpropagation training method.

1 INTRODUCTION

Simulation of hysteresis characteristics of magnetic materials needs to be implemented into electromagnetic field simulation software tools to predict the behaviour of different types of magnetic equipment. Hysteresis characteristics of magnetic materials can be described by a non-linear, multivalued relation between the magnetic field intensity $H(t)$ and the magnetization $M(t)$. That is called the hysteresis operator. Many assumptions and hypotheses have been developed since the last period of magnetic research, as the classical Preisach model [1, 2, 3, 11], the Jiles-Atherton model [1], the Stoner-Wohlfarth model [5] and some new approaches based on NNs [7, 8, 9].

A mathematical hysteresis operator with continuous output built on the function approximation ability of feedforward type NNs and its vectorial generalization for isotropic and anisotropic magnetic materials in two and three dimensions have been introduced in this paper [12–18]. The applicability of the developed method is illustrated in figures.

2 NEURAL NETWORKS FOR FUNCTION APPROXIMATION

NNs are parallel information-processing systems, implemented by hardware or software. Using the technique of NNs is a quite new and very attractive calculating method, moreover a powerful mathematical tool, because it may be applied to solve problems which conventional methods on traditional computers find difficulties to work out [10].

One of the wide pallets of applications of NNs is the function approximation, based on the theorem of Kolmogorov-Arnold. This theorem can be formulated as follows. For each positive integer n, there exist $2n+1$ continuous functions $\Phi_1, \Phi_2, \ldots, \Phi_{2n+1}$, mapping $[0, 1]$ into the real line, and having the additional property that, for any continuous function $f(x_1, x_2, \ldots, x_n)$ of n real variables, there is a continuous function Ψ of one variable on $[0, n]$ into the real line such that

$$f(x_1, x_2, \ldots, x_n) = \sum_{q=1}^{2n+1} \Psi\left\{\sum_{p=1}^{n} \Phi_q(x_p)\right\} \qquad (1)$$

for all values of $x_1, x_2, \ldots, x_n$ in the interval $[0, 1]$. There has not been any rule how to choose the functions Ψ and Φ_q, but there is a lot of latitude. Equation (1) can be represented by a feedforward type NN with at least two hidden layers with non-linear activation functions, so this type of NNs can be applied for universal function approximation.

Feedforward type NNs consist of elementary processing elements (neurons) collected into layers. The output of an individual neuron y is the output of a non-linear, differentiable activation function $y = \psi(s)$, where s is the linear combination of the input values $\boldsymbol{x}$, $s = \boldsymbol{w}^\top \boldsymbol{x} + b$, where $\boldsymbol{w}$ and b are the weight coefficients and the bias of the neuron, moreover $\psi(\cdot)$ is typically the bipolar sigmoid activation function. Neurons in the j^{th} layer are connected into the neurons in the $(j+1)^{\text{th}}$ layer by weights

* Department of Electromagnetic Theory, Budapest University of Technology and Economics Egry J. u. 18, H-1521 Budapest, Hungary, e-mail: kuczman@evtsz1.evt.bme.hu

ISSN 1335-3632

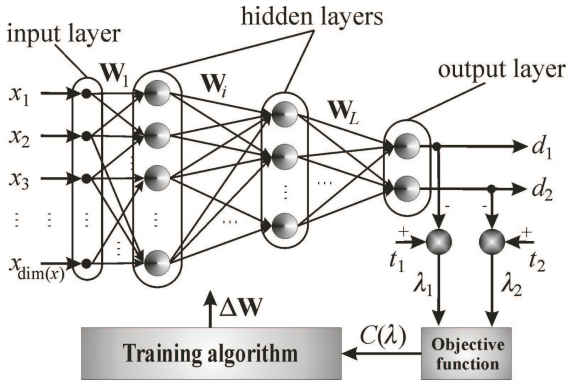

Fig. 1. Structure and training of feed-forward type NNs

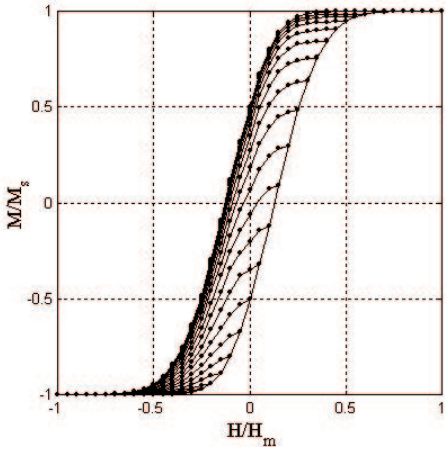

Fig. 2. A set of the first order reversal hysteresis curves

$\mathbf{W}$. If the transfer function of the individual neurons has been chosen beforehand, then the only one degree of freedom left is the setting of weights $\mathbf{W}$. These weights can be determined by a convergent, iterative algorithm, called training process to minimize a suitably defined error (mean square error, MSE, sum squared error, SSE, *etc*) between the desired output value measured on a real plant and the answer of the network. Training or adaptation is the most important property of NNs, so networks are able to modify their behaviour, to infer from imperfect, noisy and incomplete data sets. The aim of training algorithm is to modify the weights of the NN, to find an appropriate model, to create a functional relationship between input-output training patterns. Training patterns can be collected in input-output pairs in the general form $\tau^{(N)} = \{(x_k, t_k)\,,\ k = 1, \ldots, N\}$, where $t_k = f(x_k)$ and N is the number of measured points.

Mathematically, the training method is a minimization task that can be written for MISO (multi input single output) systems as

$$\mathbf{W}^*\colon \min_W \frac{1}{N}\sum_{n=1}^{N}\big(t_n - \Psi(x_n, \mathbf{W})\big)^2\,, \tag{2}$$

where $d_n = \Psi(x_n, \mathbf{W})$ is the output of NN and $\mathbf{W}$ is the weight matrix of the network. Calculation of the minimum value of the criterion function $C(\lambda)$ is realized by an iterative algorithm, $\partial C(\lambda)/\partial \mathbf{W} = \nabla\left[C(\lambda)\right] \to 0$, where λ is the normalized sum of the difference between the desired value and the output of the NN. The weights are adapted in every iteration steps k as

$$\mathbf{W}(k+1) = \mathbf{W}(k) + \Delta\mathbf{W}(k)\,. \tag{3}$$

The value of $\Delta\mathbf{W}(k)$ can be formulated in many ways. The most generally applied training method is the backpropagation algorithm, but we used a modified, faster procedure, the Levenberg-Marquardt optimization method, which uses the following adaptation rule:
$\Delta\mathbf{W} = -\big(\mathbf{J}^\top\mathbf{J} + \alpha\mathbf{I}\big)^{-1}\mathbf{J}^\top\boldsymbol{\alpha}$, where $\boldsymbol{\alpha}$ is an error vector, α is a the Levenberg parameter, $\mathbf{I}$ is the unit matrix and $\mathbf{J}$ is the Jacobian matrix of derivatives of each error to each weight. The general structure of feedforward type NNs and the supervised training algorithm can be seen in Fig. 1.

A set of experimental data $\tau^{(N)}$, measured on a real specimen must be used to execute the training algorithm. In our investigations we applied the classical scalar Preisach model for generating the training data set [2, 3].

3 THE SCALAR HYSTERESIS MODEL

The developed NN model of scalar hysteresis characteristics consists of a system of two feedforward type NNs with bipolar sigmoid transfer functions and a heuristic if-then type knowledge-base about the hysteresis phenomena.

Let us suppose that the virgin curve and a set of the first order reversal branches are available. It has been found that it is enough to use only the descending (or ascending) branches (Fig. 2) because of the symmetry of hysteresis characteristics. Hysteresis curves are normalized with the magnetization value in saturation state M_s and the appropriate magnetic field intensity, denoted by H_s. In practice, these data sets can be replaced by measurements [12–18].

Hysteresis characteristics is a multivalued function, it results in difficulties when using feedforward type NNs. If a new dimension is introduced to the measured and normalized transition curves, multivalued function can be represented by a single-valued surface. The downgrade part of hysteresis characteristics can be described at a turning point $H_{tp}^{(desc)}$ with a negative real parameter $\xi^{(desc)}$, determined as $\xi^{(desc)} = -\big(1 + H_{tp}^{(desc)}\big)/2$. The effect of this pre-processing technique can be seen in Fig. 3 for descending curves. After pre-processing, function approximation can be worked out by feedforward

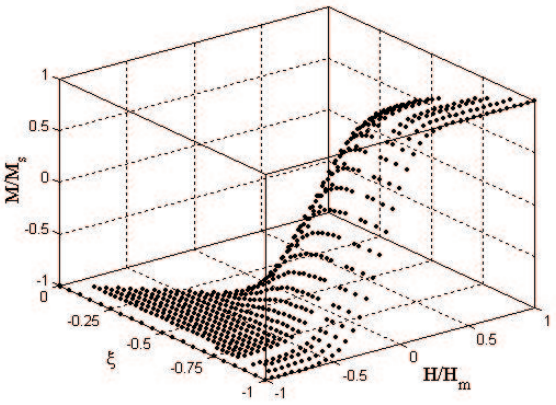

Fig. 3. First order reversal branches after preprocessing

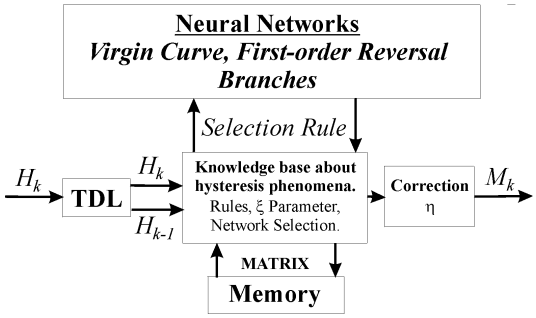

Fig. 4. Block representation of the scalar neural network model of hysteresis

type NNs trained by the Levenberg-Marquardt back-propagation method [10]. The anhysteretic curve with 41 training points can be approximated by a NN with 8 neurons in one hidden layer, and the pre-processed first order reversal branches (about 500–600 data pairs) are approached by a NN with 7, 11 and 6 processing elements in 3 hidden layers. Training of NNs takes about twenty minutes ($MSE = 5 \times 10^{-6}$) on a Celeron 566 MHz computer (192 Mbyte RAM), using the Neural Network Toolbox of MATLAB.

Applying NNs, relationship between magnetization M and magnetic field intensity H can be performed in analytical formula, $M = \mathcal{H}\{H\}$.

Memory mechanism of magnetic materials is realized by an additional algorithm based on heuristics. It is the knowledge-base for the properties of hysteresis phenomena. Magnetization at a simulation step responded by the NN is constructed on the actual value of the magnetic field intensity, the appropriate value of parameter ξ and the set of turning points. Turning points in the ascending and descending branches are stored in the memory, which is a matrix with division $[H_{tp}, M_{tp}, \xi]^\top$. Turning points can be detected by evaluation of a sequence of $\{H_{k-1}, H_k\}$ generated by a tapped delay line (TDL). After detecting a turning point $H_{tp} = H_{k-1}$ and storing it in the memory, the aim is to select an appropriate transition curve for the detected turning point calculated by the regula falsi method.

Conditions are collected in the selection rules, to choose the suitable NN. After detecting a turning point, generally denoted by $H_{START} = H_{tp}$, the algorithm for minor loops can be summarized as follows.

If $\mathbf{MATRIX}^{(desc)}$ ($\mathbf{MATRIX}^{(asc)}$) has more columns and magnetic field intensity is increasing (decreasing) at the k^{th} simulation step, the actual minor loop must be closed at the last stored value of $H_{GOAL} = H_{tp}^{(desc)}$ ($H_{GOAL} = H_{tp}^{(asc)}$) which can be found in the last column of $\mathbf{MATRIX}^{(desc)}$ ($\mathbf{MATRIX}^{(asc)}$). Denote this column of the appropriate **MATRIX** with C. The value of normalized magnetization M_k responded by the neural model at H_{GOAL} must be equal to $M_{GOAL} = M_{tp}^{(desc)}$ ($M_{GOAL} = M_{tp}^{(asc)}$) in the C^{th} column of the according **MATRIX**. It is the condition for closing the minor loops, it can be satisfied by the correction function

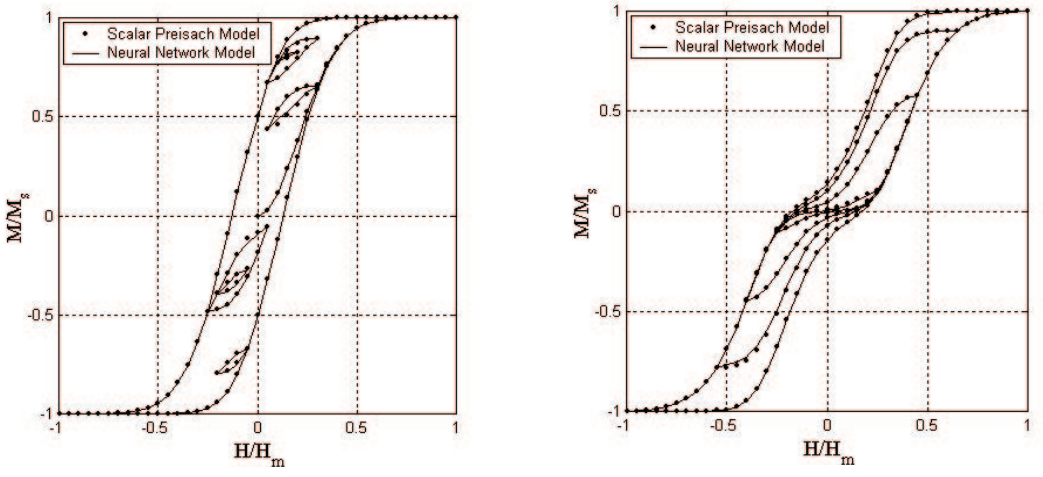

Fig. 5. Comparison of neural scalar model and the classical Preisach model

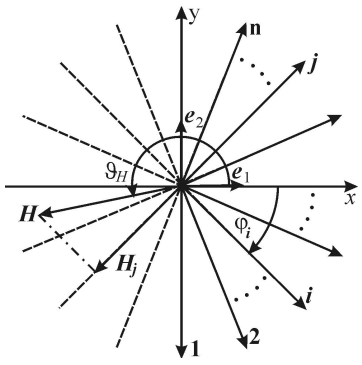

Fig. 6. Definition of directions in two dimensions

$\eta = \eta(H, M)$, where $\eta\big(H_{START}, M_{START}\big) = M_{GOAL} - M_{GOAL}^{(NN)}$ and decreasing linearly. After closing a minor loop, the appropriate columns of **MATRIX** must be erased.

The block representation of the model can be seen in Fig. 4.

The experimented NN model of hysteresis can be used as a mathematical, continuous scalar model to simulate the behaviour of magnetic materials. Two kinds of hysteresis characteristics predicted by the developed model have been compared with the results of the Preisach model as plotted in Fig. 5.

Accommodation property also can be simulated, when $H_k = H_k + \alpha M_{k-1}$ is applied as an input of the model, where α is the moving parameter [1, 11].

In electromagnetic field calculation software it is favourable to use the Newton-Raphson iteration technique. It requires the value of differential susceptibility, $\chi_{diff} = \mathrm{d}M/\mathrm{d}H$, which can be performed in analytical form by the chain rule when applying NNs, $\mathrm{d}M/\mathrm{d}H = \mathrm{d}\mathcal{H}\{H\}/\mathrm{d}H$.

4 ISOTROPIC VECTOR HYSTERESIS MODEL

The vector NN model of magnetic hysteresis is constructed as a superposition of scalar NN models in given directions $\boldsymbol{e}_\varphi$ [1, 6, 11]. The magnetization vector $\boldsymbol{M}$ can be expressed in *two dimensions* as

$$\boldsymbol{M}(t) = \int_{-\pi/2}^{\pi/2} \boldsymbol{e}_\varphi \mathcal{H}\{H_\varphi\}\mathrm{d}\varphi\,, \tag{4}$$

where $M_\varphi = \mathcal{H}\{H_\varphi\}$ is the magnetization in the direction $\boldsymbol{e}_\varphi$, $H_\varphi = |\boldsymbol{H}|\cos(\vartheta_H - \varphi)$ and ϑ_H is the direction of magnetic field intensity vector $\boldsymbol{H}$. The functions $\mathcal{H}\{H_\varphi\}$ depend on the polar angle φ if the magnetic material presents anisotropy, otherwise it is φ-independent. Firstly, isotropic case has been analyzed. In computer realization it is useful to discretize the interval $[-\pi/2, \pi/2]$ $(x \geq 0)$ as $\varphi_i = -\pi/2 + (i-1)\pi/n$, where $i = 1, \ldots, n$ (Fig. 6) and n is the number of directions.

In *three dimensions* a similar expression can be obtained,

$$\boldsymbol{M}(t) = \int_{-\pi/2}^{\pi/2}\int_{-\pi/2}^{\pi/2} \boldsymbol{e}_{\vartheta,\varphi} \mathcal{H}\{H_{\vartheta,\varphi}\}\mathrm{d}\vartheta\mathrm{d}\varphi\,. \tag{5}$$

where

$$H_{\vartheta,\varphi} = [\,a_1 \quad a_2 \quad a_3\,]_{\vartheta,\varphi}\,[\,H_x \quad H_y \quad H_z\,]^\top\,, \tag{6}$$

and the directions are given as $\boldsymbol{a} = a_1\boldsymbol{e}_1 + a_2\boldsymbol{e}_2 + a_3\boldsymbol{e}_3$, $|\boldsymbol{a}| = 1$. Directions of the three dimensional model are generated by the icosahedron. The angles φ and ϑ are measured from the x-axis and the x–y plane.

After measuring the Everett surface in the x direction, the following expression can be obtained between the measured scalar Everett surface $F(\alpha, \beta)$ and the unknown vector Everett function $E(\alpha, \beta)$:

$$F(\alpha, \beta) \cong \sum_{i=1}^{n} \cos\varphi_i E(\alpha\cos\varphi_i, \beta\cos\varphi_i)\,. \tag{7}$$

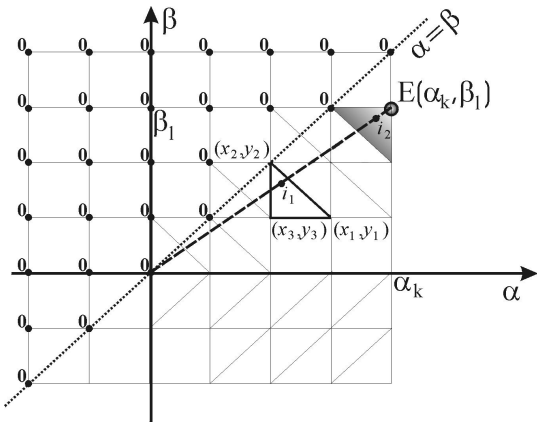

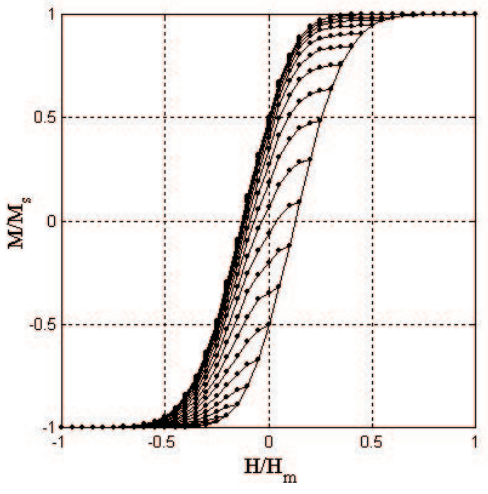

Fig. 7. Illustration for the identification process

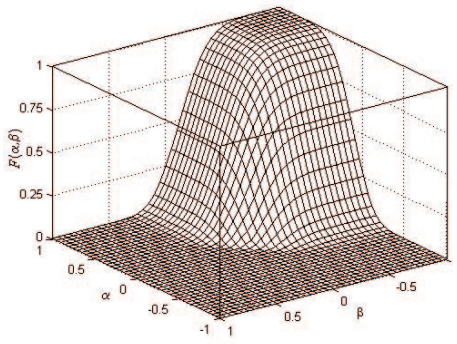

Fig. 8. First order reversal curves of hysteresis and the Everett surface measured in the x direction

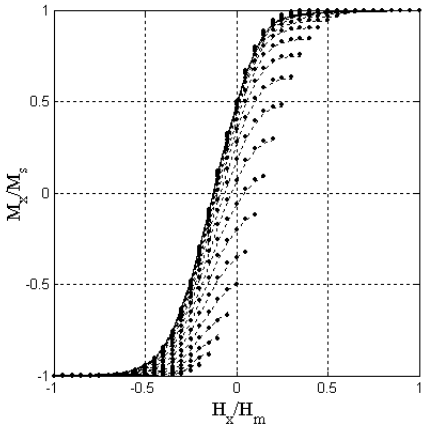

Fig. 9. The resulted identification in two dimensions for isotropic case

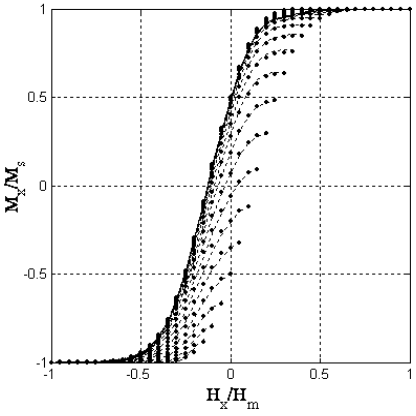

Fig. 10. The resulted identification in three dimensions for isotropic case

In an isotropic case the vector Everett surface is unique for all directions. Expression (7) can be solved numerically, the algorithms is given as follows. The formulation (7) can be rewritten in the form

$$F(\alpha_k,\beta_l) \cong \sum_{i_1=1}^{n_1} \cos\varphi_{i_1}\, E(\alpha_k\cos\varphi_{i_1}, \beta_l\cos\varphi_{i_1}) + \sum_{i_2=1}^{n_2} \cos\varphi_{i_2}\, E(\alpha_k\cos\varphi_{i_2}, \beta_l\cos\varphi_{i_2})\,, \quad (8)$$

where $\alpha_k = 2\big(k-(N+2)/2\big)$, $\beta_l = 2\big((N+2)/2-l\big)/N$, $k,l = 1,\ldots,N+1$ and the size of the Everett table is $(N+1)\times(N+1)$. Expression (8) contains n_1 known and n_2 unknown points in the Everett surface (Fig. 7). The first sum contains known values of the Everett function, $E(\alpha_k\cos\varphi_{i_1}, \beta_l\cos\varphi_{i_1})$ because $\alpha_{j-1} \le \alpha_k\cos\varphi_{i_1} \le \alpha_j$ and $\beta_m \le \beta_l\cos\varphi_{i_1} \le \beta_{m-1}$ $(m-1>l,\ j<k)$. The second sum contains the unknown value of the vector Everett surface.

If $\beta_l = 0$, $l = 1,\ldots,N+1$ and assuming linear interpolation in the surface $E(\alpha,\beta)$, the

$$F(\alpha_k,0) = \sum_{i_1=1}^{n_1} \Big(\cos\varphi_{i_1}\big(E(\alpha_{j-1},0) + \big(E(\alpha_j,0) - E(\alpha_{j-1},0)\big)(\alpha_k\cos\varphi_{i_1}-\alpha_{j-1})/(\alpha_j-\alpha_{j-1})\big)\Big) + E(\alpha_{k-1},0)\big((1+b_k)c_1 - a_k c_2\big) + E(\alpha_k,0)(a_k c_2 - b_k c_1)\,, \quad (9)$$

formulation can be got, where $c_1 = \sum_{i_2=1}^{n_2}\cos\varphi_{i_2}$, $c_2 = \sum_{i_2=1}^{n_2}\cos^2\varphi_{i_2}$, $a_k = \alpha_k/(\alpha_k-\alpha_{k-1})$, $b_k = \alpha_{k-1}/(\alpha_k-\alpha_{k-1})$ and $j \le k-1$. From (9), value of $E(\alpha_k,0)$ can be expressed. A similar relation can be obtained, when $\alpha_k = \beta_k$.

If $\beta \ne 0$, a similar mathematical formulation can be obtained. Firstly, let us assume that $(\alpha_k\cos\varphi_{i_1}, \beta_l\cos\varphi_{i_1})$ is bounded by known points $A(x_1,y_1,z_1)$, $B(x_2,y_2,z_2)$ and $C(x_3,y_3,z_3)$ in the vector Everett surface. The value of the Everett surface in this co-ordinate can be expressed assuming linear interpolation in the given triangle (A,B,C). Unknown values can be expressed after some simple mathematical formulations using linear interpolation in a triangle.

Because of symmetry of the hysteresis characteristics, it is enough to calculate the half of the Everett surface.

First order reversal curves of vector NN model can be calculated from the identified vector Everett surface as $M_{\alpha\beta} = M_\alpha - 2E(\alpha,\beta)$, where M_α is a reversal magnetization point in the major hysteresis loop according to the magnetic field intensity α, and $M_{\alpha\beta}$ is a magnetization value in a reversal curve starting from the reversal point (α, M_α). The reversal curves can be approximated by the scalar NN model.

Let us assume that the measured hysteresis curve and the corresponding Everett surface are given in the x direction as plotted in Fig. 8.

Simulation results for reversal curves obtained from the identified Everett surface in two dimensions (20 directions) and three dimensions (24 directions) can be seen

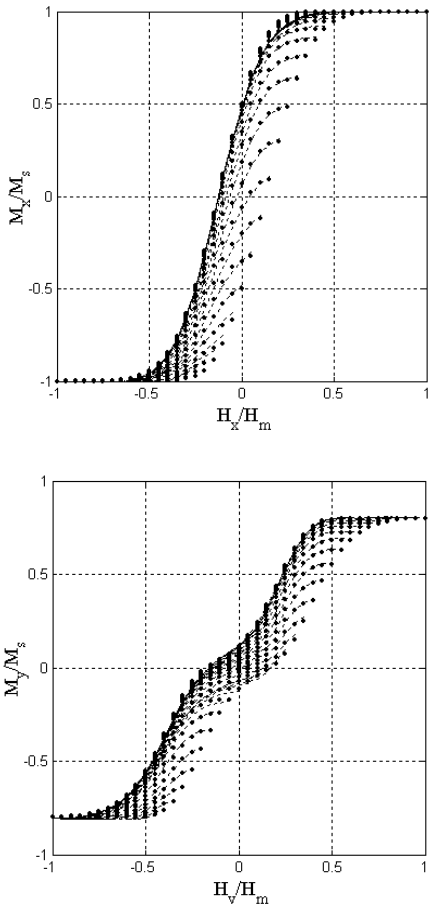

Fig. 11. Identification results in two dimensions for anisotropic case, (a) in the easy axis and (b) in the hard axis

in Fig. 9 and Fig. 10. Experimental results are denoted by points, hysteresis characteristics given by the NN model is denoted by the dashed line.

5 ANISOTROPIC VECTOR HYSTERESIS MODEL

In an anisotropic case the scalar Everett surface is depending on the direction φ [1, 6, 11]. It is difficult to take into account the angular dependence of the Everett surface in the identification task, therefore the Fourier expansion has been applied, so the same identification procedure can be used as in the isotropic case. In two dimensions, the Everett surface $F(\varphi) = F(\alpha, \beta, \varphi)$ is π-periodic with respect to φ and an even function $F(-\varphi) = F(\varphi)$ if $\varphi = 0$ and $\varphi = \pi/2$ represents the easy axis and the hard axis. Let us assume that the Everett functions are available in n directions in the interval $[0, \pi/2]$ from measurements using the Epstein's frame. The angular dependence of the Everett surface can be handled by the Fourier expansion as

$$F(\varphi) \cong \sum_k C_k \cos(2k\varphi)\,, \tag{10}$$

where function $C_k = C_k(\alpha, \beta)$ is the k^{th} harmonic component, which is independent of the angle φ. Using the trapezoidal formula for integration, the Fourier components can be calculated as

$$C_0 = \frac{\Delta\varphi}{\pi}\Big(\big(F(0) + F(\pi/2)\big) + 2\sum_{i=1}^{n-1} F(\varphi_i)\Big) \tag{11}$$

and

$$C_k = \frac{2\Delta\varphi}{\pi}\Big(\big(F(0) + F(\pi/2)(-1)^k\big) + 2\sum_{i=1}^{n-1} F(\varphi_i)\cos(2k\varphi_i)\Big) \tag{12}$$

where $\Delta\varphi = \pi/\big(2(n-1)\big)$. The same identification process can be applied as in the isotropic case for the Fourier harmonics,

$$C_k(\alpha, \beta) \cong \sum_{i=1}^{n'} \cos\varphi_i \cos(2k\varphi_i) E_k(\alpha\cos\varphi_i, \beta\cos\varphi_i)\,, \tag{13}$$

where $\varphi_i = -\pi/2 + (i-1)\pi/n'$ and $n' = 2(n-1)$ is the number of directions. In this study two angular harmonics ($k = 0,\ 1$) have been used.

In *three dimensions* a similar process can be applied. Assuming the same conditions as in 2D model, the Everett surface $F(\vartheta, \varphi) = F(\alpha, \beta, \vartheta, \varphi)$ also can be represented by a Fourier expansion with respect to ϑ and φ in the form

$$F(\vartheta, \varphi) \cong \sum_n \sum_m C_{mn} \cos(2m\vartheta)\cos(2n\varphi)\,, \tag{14}$$

where function $C_{mn} = C_{mn}(\alpha, \beta)$ is the harmonic component, and can be calculated as

$$\begin{aligned} C_{00} &= \frac{4}{\pi^2}\int_0^{\pi/2}\int_0^{\pi/2} F(\vartheta, \varphi)\mathrm{d}\vartheta\mathrm{d}\varphi \cong \frac{\Delta\vartheta\,\Delta\varphi}{\pi^2}\Big(\big(F(0,0) \\ &+ F(\pi/2, 0) + F(0, \pi/2) + F(\pi/2, \pi/2)\big) + 2\sum_{k=1}^{M-1}\big(F(\vartheta_k, 0) \\ &+ F(\vartheta_k, \pi/2)\big) + 2\sum_{l=1}^{N-1}\big(F(0, \varphi_l) + F(\pi/2, \varphi_l)\big) \\ &+ 4\sum_{k=1}^{M-1}\sum_{l=1}^{N-1} F(\vartheta_k, \varphi_l)\Big) \end{aligned} \tag{15}$$

and

$$\begin{aligned} C_{mn} &= \frac{8}{\pi^2}\int_0^{\pi/2}\int_0^{\pi/2} F(\vartheta, \varphi)\cos(2m\vartheta)\cos(2n\varphi)\mathrm{d}\vartheta\mathrm{d}\varphi \\ &\cong \frac{2\Delta\vartheta\,\Delta\varphi}{\pi^2}\Big(\big(F(0,0) + F(\pi/2, 0)(-1)^m + F(0, \pi/)(-1)^n \\ &+ F(\pi/2, \pi/2)(-1)^{m+n}\big)\Big) \\ &+ 2\sum_{k=1}^{M-1}\big(F(\vartheta_k, 0) + F(\vartheta_k, \pi/2)(-1)^n\big)\cos(2m\vartheta_k) \\ &+ 2\sum_{l=1}^{N-1}\big(F(0, \varphi_l) + F(\pi/2, \varphi_l)(-1)^m\big)\cos(2n\varphi_l) \\ &+ 4\sum_{k=1}^{M-1}\sum_{l=1}^{N-1} F(\vartheta_k, \varphi_l)\cos(2m\vartheta_k)\cos(2n\varphi_l)\,, \end{aligned} \tag{16}$$

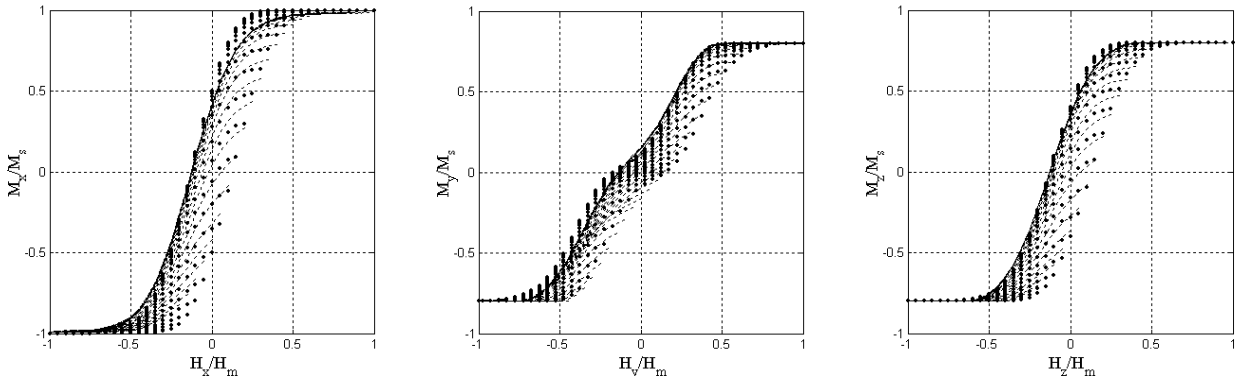

Fig. 12. Identification results in three dimensions for anisotropic case, (a) in the x, (b) in the y and (c) in the z directions

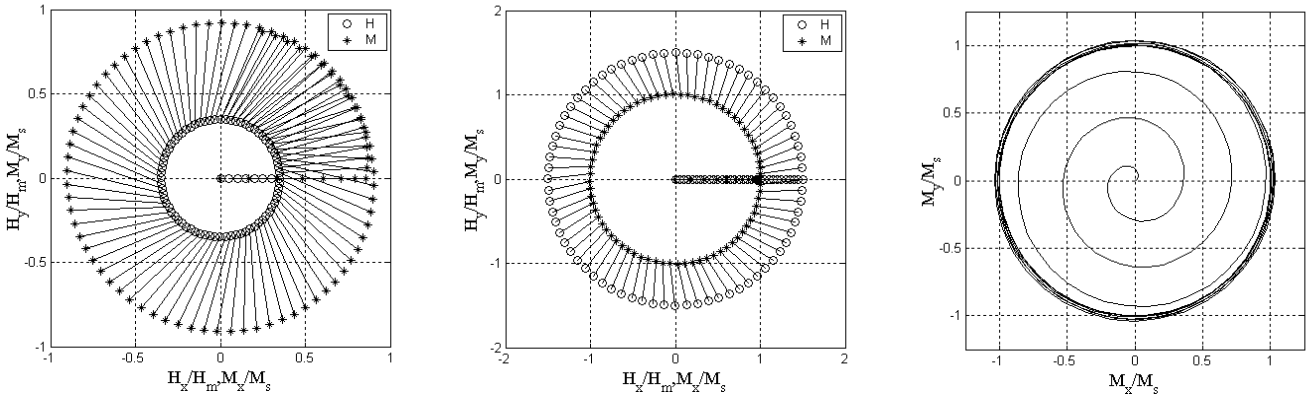

Fig. 13. Simulated H and M loci for different conditions in isotropic case

where $\vartheta \in [0, \pi/2]$, $\varphi \in [0, \pi/2]$ $\Delta\vartheta = \pi/\big(2(M-1)\big)$ and $\Delta\varphi = \pi/\big(2(N-1)\big)$. In this case $M \times N$ measurements must be used.

The identification process must be applied for the following expression:

$$C_{mn}(\alpha,\beta) \cong \sum_{i=1}^{n'} \cos\psi_i \cos(2m\vartheta_i)\cos(2n\varphi_i) \times E_{mn}(\alpha\cos\psi_i, \beta\cos\psi_i)\,, \quad (17)$$

where n' is the number of directions generated by the icosahedron and ψ_i is the angle between the i^{th} direction given by the icosahedron and the x-axis. In this study two angular harmonics according to the angles ϑ and φ $(m, n = 0,\, 1)$ have been used.

After the identification process, the Everett surfaces in the given directions can be calculated similarly to the expression (10) in two dimensions or equation (14) in three dimensions. Knowing the Everett surfaces, first order reversal curves can be generated and NNs can be trained.

The introduced methods have been applied to simulate anisotropic magnetic materials. In two dimensions ten different scalar hysteresis characteristics were available, generated by the elliptical interpolation function

$$F(\varphi) = F_x^2 \cos^2\varphi + F_y^2 \sin^2\varphi\,, \quad (18)$$

where $F(\varphi) = F(\alpha,\beta,\varphi)$ and $F_x = F_x(\alpha,\beta,\varphi)$, $F_y = F_y(\alpha,\beta,\varphi)$ are the known Everett surfaces in the rolling and transverse directions and $\varphi \in [0, \pi/2]$ [4]. In three dimensions 5×5 scalar hysteresis characteristics have been assumed, constructed by the expression

$$F(\vartheta,\varphi) = \cos^2\vartheta(F_x^2\cos^2\varphi + F_y^2\sin^2\varphi) + F_z^2\sin^2\vartheta\,, \quad (19)$$

where $F(\vartheta,\varphi) = F(\alpha,\beta,\vartheta,\varphi)$, and $F_x = F_x(\alpha,\beta,\vartheta,\varphi)$, $F_y = F_y(\alpha,\beta,\vartheta,\varphi)$, $F_z = F_z(\alpha,\beta,\vartheta,\varphi)$ are the known Everett surfaces in the x, y and z axis. In practice, these data sets can be replaced by measurements with the usual Epstein's frame.

Simulation results for reversal curves obtained from the identified Everett surface in two dimensions (18 directions) and three dimensions (9 directions) can be seen

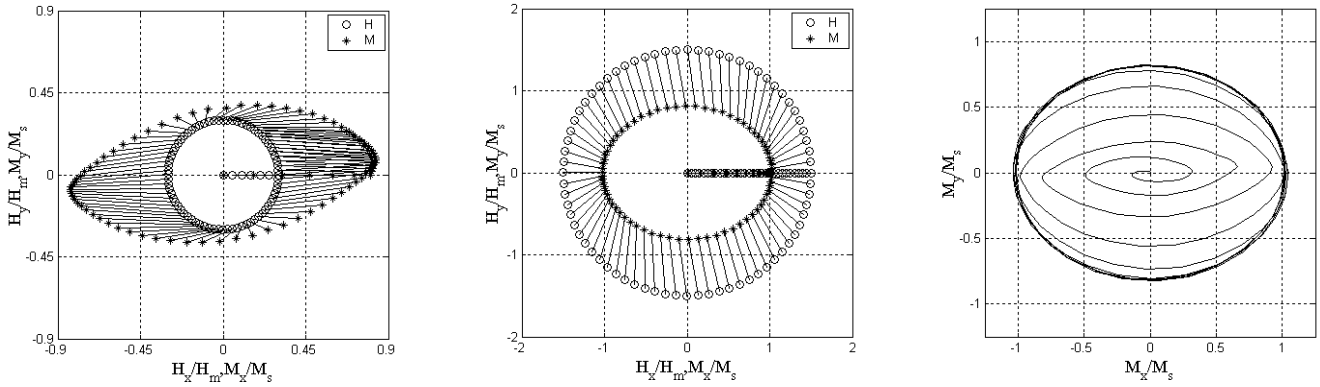

Fig. 14. Simulated H and M loci for different conditions in anisotropic case

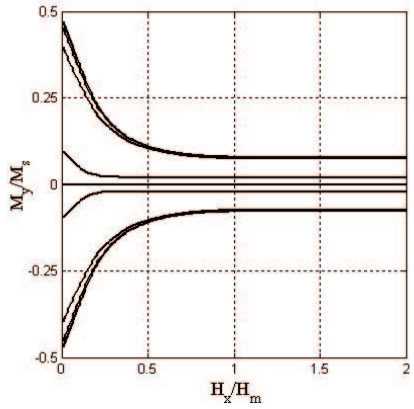

Fig. 15. Induced anisotropy in isotropic material

in Fig. 11.a,b and Fig. 12.a, b, and c (trivial conditions in the directions of x, y and z axes). Experimental results are denoted by points, hysteresis characteristics given by the NN model is denoted by the dashed line.

6 SOME PROPERTIES OF THE NN VECTOR MODEL

Applying rotational magnetic field intensity with different amplitude and with linearly increasing amplitude, the output of the 2D vector NN isotropic model has been plotted in Fig. 13. a, b and c. The specimen is magnetized to a given value in the rolling direction, and then the magnetic field intensity is rotated keeping its magnitude constant (Fig. 13. a and b). In Fig. 13.c, the vector of magnetization gradually approaches the regime of uniform rotation. The variation of the circular polarized magnetic field intensity is the following:

$$\boldsymbol{H}(t) = \big\{H_x(t) = H_m \cos(\omega t)\,,\; H_y(t) = H_m \sin(\omega t)\big\}, \quad (20)$$

where H_m is the amplitude of magnetic field intensity and ω is the angular velocity [11]. The results for 2D anisotropic vector model under the same conditions can be seen in Fig. 14. a, b and c. These figures highlight the anisotropic material behaviour.

Let us suppose that the magnetic field intensity was first increased along the y direction of the isotropic magnetic material to a given value, and then it was decreased to zero. This process results in remanent magnetization in y direction. After reaching H_y zero, magnetic field intensity is increased along the x direction. The orthogonal remanent component of magnetization can be reduced as it can be seen in Fig. 15 for different remanent values. It is an anisotropy induced by the magnetic prehistory of the material [4, 11].

The position of the vector of magnetization and the hysteresis loops along the x and y-axis for a linear excitation in anisotropic case are plotted in Fig. 16 a, b and c.

7 CONCLUSIONS

A NN model for magnetic hysteresis based on the function approximation ability of NNs has been experimented. The anhysteretic magnetization curve and a set of the first order reversal branches must be measured on a real magnetic material. Introducing an additional parameter ξ solves a fundamental problem of simulating hysteresis characteristics, that is the multivalued property. The magnetization becomes a single valued function of two variables and an if-then type knowledge-base can be used for simulating different phenomena of magnetic materials.

This method has been generalized in two and three dimensions with an original identification process. The vector model is based on the Mayergoyz type technique, but identical scalar models are constructed on the identified scalar NN model of hysteresis.

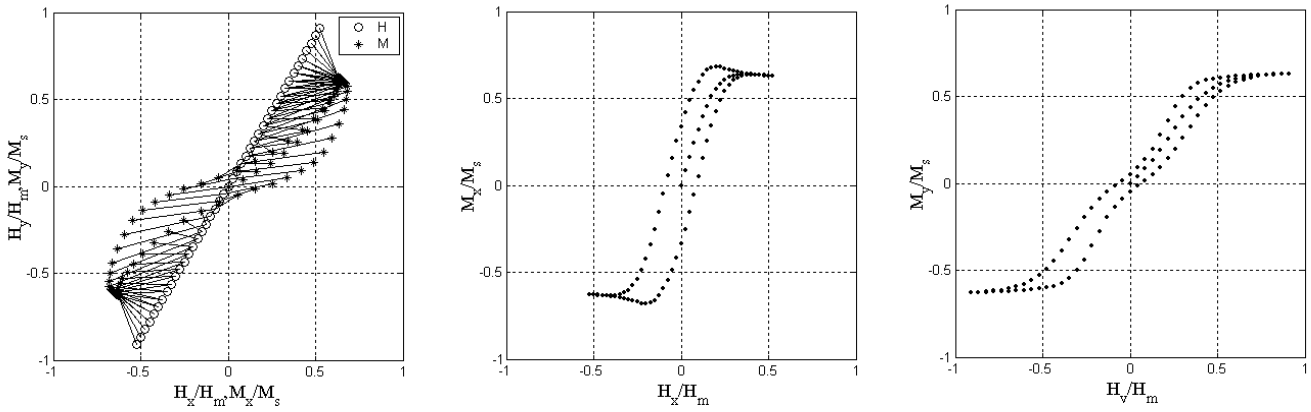

Fig. 16. Anisotropic magnetic material in linear excitation, (a) vector of H and M, (b) hysteresis characteristics in the x-axis and (c) in the y-axis

Acknowledgement.

The research work is sponsored by the Hungarian Scientific Research Fund, OTKA 2002, Pr. No. T 034 164/2002.

References

[1] IVÁNYI, A.: Hysteresis Models in Electromagnetic Computation, Akadémia Kiadó, Budapest, 1997.

[2] FÜZI, J.: Parameter Identification in Preisach Model to Fit Major Loop Data, in Applied Electromagnetics and Computational Technology, in Series of Studies in Applied Electromagnetics and Mechanism, vol. 11, IOS Press, 1997, pp. 77–82.

[3] FÜZI, J.—HELEREA, E.—OLTENAU, D.—IVÁNYI, A.—PFÜTZNER, H.: Experimental Verification of a Preisach-Type Model of Magnetic Hysteresis, Studies in Applied Electromagnetics and Mechanics,, vol. 13 Non-linear Electromagnetic Systems 8th ISEM Conference Braunschweig, IOS Press, 1997, pp. 479–482.

[4] FÜZI, J.—IVÁNYI, A.: Isotropic Vector Preisach Particle, Physica B **275** (2000), 179–182.

[5] SZABÓ, Zs.—IVÁNYI, A.: Computer-Aided Simulation of Stoner-Wohlfarth Model, Journal of Magnetism and Magnetic Materials **215-216** (2000), 33–36.

[6] RAGUSA, C.—REPETTO, M.: Accurate Analysis of Magnetic Devices with Anisotropic Vector Hysteresis, Physica B **275** (2000), 92–98.

[7] SERPICO, C.—VISONE, C.: Magnetic Hysteresis Modeling via Feed-Forward Neural Networks, IEEE Trans. on Magn. **34** (1998), 623–628.

[8] ADLY, A.A.—ABD-El-HAZIF, S.K.: Using Neural Networks in the Identification of Preisach-Type Hysteresis Models, IEEE Trans. on Magn. **34** (1998), 629–635.

[9] ADLY, A.A.—ABD-El-HAZIF, S.K.—MAYERGOYZ, I.D.: Identification of Vector Preisach Models from Arbitrary Measured Data Using Neural Networks, Journal of Applied Physics **87** No. 9 (2000), 6821–6823.

[10] CHRISTODOULOU, C.—GEORGIOPOULOS, M.: Applications of Neural Networks in Electromagnetics, Artech House, Norwood, 2001.

[11] MAYERGOYZ, I. D.: Mathematical Models of Hysteresis, Springer, 1991.

[12] KUCZMANN, M.—IVÁNYI, A.: Scalar Hysteresis Model Based on Neural Network, IEEE International Workshop on Intelligent Signal Processing, Budapest, Hungary, May 24–25, 2001, pp. 143–148.

[13] KUCZMANN, M.—IVÁNYI, A.: Vector Neural Network Hysteresis Model, Physica B **306** (2001), 143–148.

[14] KUCZMANN, M.—IVÁNYI, A.: A New Neural Network Based Scalar Hysteresis Model, Record of the 13th Compumag Conference on the Computation of Electromagnetic Fields, Lyon-Evian, France, July 2-5, 2001, vol. 2/4, PC1-9, pp. 30–31.

[15] KUCZMANN, M.—IVÁNYI, A.: Neural Network Based Scalar Hysteresis Model, Proceedings of the 10th International Symposium on Applied Electromagnetics and Mechanics, Tokyo, Japan, May 13-16, 2001, pp. 493–494.

[16] KUCZMANN, M.—IVÁNYI, A.: Scalar Neural Network Hysteresis Model, Proceedings of the XI. International Symposium on Theoretical Electrical Engineering, Linz Austria, August 19-22, 2001, ISTET131.

[17] KUCZMANN, M.—IVÁNYI, A.—BARBARICS, T.: Neural Network Based Simulation of Scalar Hysteresis, Proceedings of the X. International Symposium on Electromagnetic Fields in Electrical Engineering, Cracow, Poland, September 20-22, 2001, pp. 413–416.

[18] KUCZMANN, M.—IVÁNYI, A.: Neural Network Model of Magnetic Hysteresis, submitted to Compel, 2002.

Received 22 November 2002

Miklós Kuczmann, obtained diploma in electrical engineering at the Budapest University of Technology and Economics in 2000. He joined the Department of Electromagnetic Theory as PhD student. His research field is the simulation of magnetic materials applying neural networks and soft computing methods, electromagnetic field calculation and nondestructive testing. He got the price of SIEMENS for diploma thesis.

Amália Iványi. Biography not supplied.